The effect of gas environment on electrical heating in suspended carbon nanotubes

I-Kai Hsu,[1] Michael T. Pettes,[3] Mehmet Aykol,[2] Li Shi,[3] and Stephen B. Cronin[2,a)]
[1]*Department of Materials Science, University of Southern California, Los Angeles, California 90089, USA*
[2]*Department of Electrical Engineering, University of Southern California, Los Angeles, California 90089, USA*
[3]*Department of Mechanical Engineering and Center for Nano and Molecular Science and Technology, Texas Materials Institute, University of Texas of Austin, Austin, Texas 78712, USA*

(Received 13 April 2010; accepted 5 September 2010; published online 21 October 2010)

We report micro-Raman spectroscopy measurements of the temperature distribution of current-carrying, 5 μm long, suspended carbon nanotubes in different gas environments near atmospheric pressure. At the same heating power, the measured *G* band phonon temperature of the nanotube is found to be significantly lower in gaseous environments than in vacuum. Theoretical analysis of these results suggests that about 50%–60% of the heat dissipated in the suspended nanotube is removed by its surrounding gas molecules, and that the thermal boundary conductance is higher in carbon dioxide than in nitrogen, argon, and helium, despite the lower thermal conductivity of carbon dioxide. © *2010 American Institute of Physics*. [doi:10.1063/1.3499256]

I. INTRODUCTION

Thermal management in nanoelectronic devices has become an important area of study because of the enormous power densities dissipated in these devices. In fact, self heating is one of the main factors limiting the performance and reliability of nanoelectronic devices fabricated using conventional materials such as silicon and copper as well as new materials including carbon nanotubes (CNTs), which possess superior electronic, mechanical, and thermal properties.[1–3] Recently, energy dissipation from current-carrying CNTs has been studied by several groups. Current saturation at high electric fields was observed in metallic CNTs supported on silicon/silicon dioxide (Si/SiO_2) substrates and was attributed to the emission of hot optical phonons by energetic electrons.[4] Negative differential conductance at high fields was measured in suspended metallic CNTs and was believed to be caused by the generation and absorption of optical phonons by electrons.[5] With the use of micro-Raman spectroscopy measurements, nonequilibrium optical phonon populations in both suspended and supported metallic CNTs were directly revealed and explained by the preferential coupling of hot electrons to different optical phonon populations.[6,7] In scanning thermal microscopy measurements of the lattice temperature distribution of current-carrying CNT devices supported on SiO_2, the majority of the Joule heat was found to be dissipated to the two contact electrodes in a multiwalled CNT and to the substrate directly in a current-carrying single-walled (SW) CNT.[8] Hence, the more pronounced hot phonon effects observed by transport and Raman measurements in suspended SWCNTs can be attributed to the elimination of the heat dissipation path to the substrate. Moreover, the high-bias current in suspended SWCNTs was measured to increase with the presence of gas molecules surrounding the nanotube in comparison to the case in vacuum. In particular, polyatomic gas molecules with lower thermal conductivity were found to lead to higher current than monatomic gases. These results could not be explained purely by heat dissipation from the nanotube to the surrounding molecules based on the maximum nanotube-gas thermal boundary conductance (g) calculated from the kinetic theory and was instead attributed to the relaxation of hot optical phonons by surrounding molecules, especially polyatomic gas molecules, due to the coupling of the molecular vibration with surface phonons.[9]

The heat dissipation from suspended CNTs to surrounding gases has been considered to be negligible in several prior measurements of the thermal properties and optical absorption of CNTs.[10–13] This assumption is justified if the thermal conductivity of the CNT samples is as high as the high-quality samples measured by other methods in vacuum and if heat transfer from CNTs to the surrounding gas molecules is not much higher than that predicted by a number of theories. In a molecular dynamics study, Hu *et al.*[14] calculated the thermal boundary conductance between a SW CNT and air at room temperature and atmospheric pressure to be about 9×10^4 W/m^2 K when the oxygen adsorption energy is taken to be 2.64 k_bT, where k_b is the Boltzmann constant. This value is close to the upper limit calculated from the kinetic theory for a molecular accommodation coefficient of unity, i.e., $g_{max}=nv_{rms}C_v/4=1.1\times10^5$ W/m^2 K,[15] in which n, v_{rms}, and C_v are the molecular density, root mean square velocity, and specific heat per molecule of the gas molecules, respectively. Here, $v_{rms}=(3\ k_BT/m)^{1/2}$, where k_B is the Boltzmann constant, T is the absolute temperature, and m is the molecule mass. For diatomic air molecular, $C_v=2.5\ k_B$. However, these theoretical calculations have not been verified experimentally by direct measurements of heat transfer between CNTs and surrounding gases.

In this work, we report an optical measurement technique coupled with an electrical heating method to study the effect of gas molecules on electron transport and heat dissi-

a)Electronic mail: scronin@usc.edu.

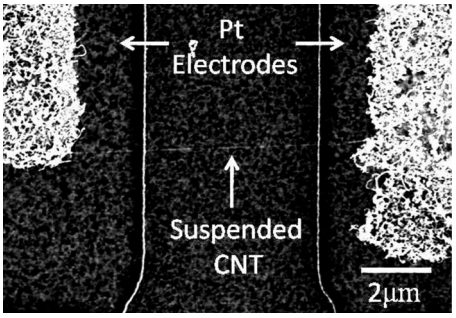

FIG. 1. SEM image of a 5 μm long CNT suspended between two Pt electrodes.

pation from current-carrying suspended CNTs. The temperature profiles of current-carrying CNTs are obtained from the *G* band Raman downshifts observed under different electrical heating powers and gaseous environments. Our measurement results show that the Raman *G* band temperature of CNTs is lowered considerably by surrounding gas molecules, which could remove a large fraction of the Joule heat for the 1–5 μm CNT samples measured here.

II. EXPERIMENTAL METHODS AND RESULTS

SWNTs were grown by chemical vapor deposition and suspended across two platinum (Pt) electrodes separated by trenches ranging from 1–5 μm wide, etched in a Si/SiO_2 substrate. The details of the sample fabrication and CNT growth process are described in a previous publication.[16] Figure 1 shows the scanning electron microscope (SEM) image of a 5 μm long CNT device measured in this study. All electrical measurements are performed with an Agilent 4156C parameter analyzer. A 532 nm Spectra-Physics solid state laser is collimated and focused through a Leica *DM*LM microscope with 40× and 100× objective lenses for measurements performed in vacuum and gaseous environments, respectively. Raman spectra of CNTs are collected in a Renishaw *inVia* Raman microspectrometer with a PRIOR ProScan II high precision microscope stage to control the position of the incident laser with respect to the CNTs. In addition, a cylindrical lens is placed in the laser beam path to create an elongated laser profile through the 100× objective lens to enable the Raman spectra along the entire 5 μm long CNT to be measured simultaneously with 0.5 μm spatial resolution. The diameter (d) of the CNT is determined from the measured radial breathing mode to be 2.04 nm.[17]

In this work, the temperature profiles along suspended CNTs are determined from the temperature-induced downshifts in *G* band Raman spectra measured with and without electrical heating current. The temperature-induced *G* band downshifts are calibrated in a Linkam THMSE 600 temperature controlled stage, revealing a value of $-0.0255\ cm^{-1}/K$, which is consistent with previous values in the literature.[10,11,16,18,19] The current-voltage (I-V) characteristics, shown in Fig. 2(a), exhibit a slight nonlinearity with a decreasing dI/dV with increasing V, which is a signature of current saturation at high fields.[4] However, we do not observe negative differential conductance.[5] The identical spatial temperature increase in G_+ and G_- phonon bands, as shown in Fig. 2(b), indicates thermal equilibrium among different phonon bands in our measurement. The two-probe resistance of this sample is on the order of 1 MΩ, indicating additional scattering due to defects and/or large contact resistances. Although the measured current appears to be slightly higher in gases than in vacuum for high-bias voltages, the measured current at the same voltage is lower in Ar and He for $V < \sim 0.8$ V and in N_2 and CO_2 for $V < 1$ V than in vacuum. The I-V characteristics of some measured samples are found to change after several electrical heating cycles, which is likely due to CNT or contact annealing. However, the order of heat removal ability among these four gases from CNTs is not affected by the variation in I-V characteristics.

Figure 3(a) shows an approximately parabolic Raman *G* band temperature (T) profiles along the axial direction (x) of the nanotube measured in vacuum at different electrical heating powers of 0.53, 0.69, and 0.87 μW. Because ballistic phonon transport would lead to a uniform temperature profile, the parabolic temperature profiles observed in Fig. 3(a) indicate the diffusive nature of the phonon transport in the CNT measured here.[10]

Figure 3(b) shows the spatial temperature data taken from the same CNT in argon at various electrical heating powers. As compared with vacuum, the heating power required to achieve the same temperature in the CNT in argon is 3.87 times larger than that required in vacuum [Fig. 3(c)].

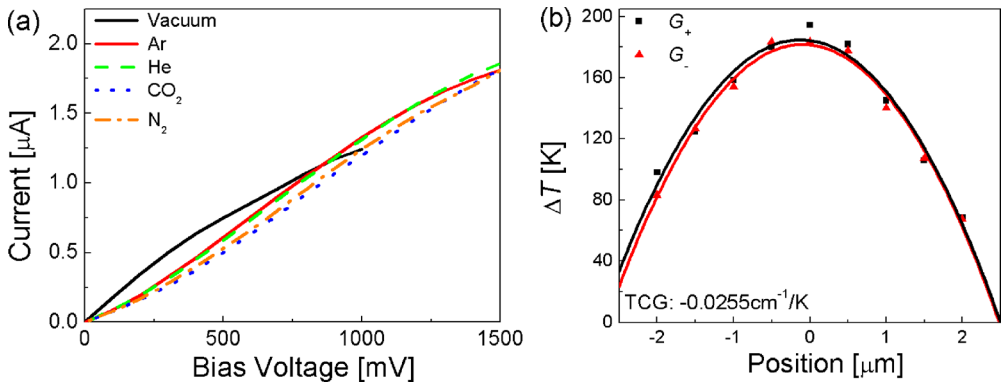

FIG. 2. (Color online) (a) Current-voltage curves of a 5 μm long suspended CNT measured in vacuum and different gas environments. (b) G_+ and G_- band phonon temperature distributions measured along the suspended CNT in argon under an electrical power of 2.67 μW. The average G_+ and G_- band phonon temperatures are 127 K and 123 K, respectively, along the suspended nanotube.

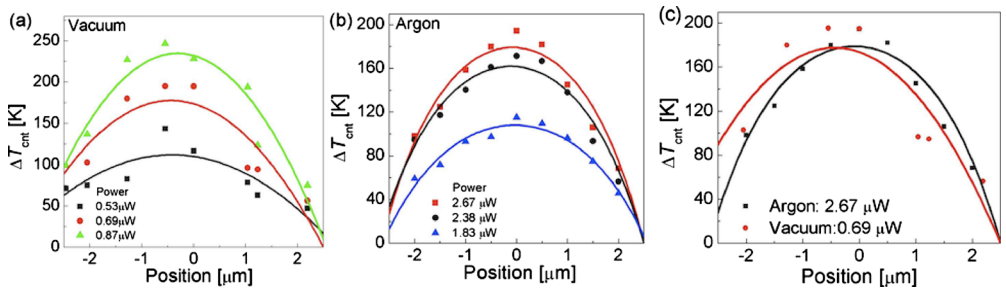

FIG. 3. (Color online) Temperature profiles along the CNT measured in Fig. 2 under various electrical heating powers (a) in vacuum and (b) in argon. (c) Comparison of heating powers required in argon and in vacuum to achieve approximately the same temperature in the nanotube.

Figure 4 shows the relation between the average temperature increase and the electrical input power of the CNT measured in different gases and vacuum. Significantly lower temperatures are observed in gases than in vacuum. Moreover, the temperatures observed in CO_2 are considerably lower than in Ar, He, and N_2 (Fig. 4), despite the fact that He has the highest thermal conductivity among these four gases. The same behavior has been observed in four other nanotubes with shorter suspended lengths $L=1-2$ μm.

Assuming local thermal equilibrium between different phonon populations, the measured temperature profile can be obtained from the heat diffusion equation

$$\frac{\partial^2 \Delta T}{\partial x^2} = -\frac{Q}{\kappa AL} + \frac{g\pi d}{\kappa A}\Delta T, \tag{1}$$

where Q, k, L, and A are the Joule heating, thermal conductivity, length, and cross sectional area in the suspended segment of the CNT. Following Ref. 20, we calculate $A=\pi d\delta$, where $\delta=0.34$ nm is the interlayer spacing of graphite.

In vacuum with radiation heat loss ignored, $g=0$ and the obtained temperature profile is quadratic. We obtain the $\partial^2\Delta T/\partial x^2$ value from a quadratic fitting of the measured temperature profiles in vacuum. Due to electrical contact resistance, the actual Joule heating in the nanotube, Q, will be lower than the measured total electrical heating power, IV, by a factor α. The $\partial^2\Delta T/\partial x^2$ value obtained in vacuum can be used to determine the $\beta \equiv k/\alpha$ ratio from Eq. (1) with $g=0$. Note that $0<\alpha\leq 1$, with the upper limit given by the case of negligible contact electrical resistance. As shown in Fig. 5, the obtained k/α shows a linear dependence on $\langle \Delta T_{cnt}\rangle^{-0.657}$, where $\langle \Delta T_{cnt}\rangle$ is the average measured temperature rise in the CNT. This feature suggests that umklapp phonon-phonon scattering is dominant in the CNT, further confirming the diffusive nature of phonon transport in this likely defective CNT.

The much lower temperature rise measured in gas environments suggests a large fraction of heat transfer to the surrounding gases compared to that of heat conducted along the CNT to the two electrodes. For $g>0$, the solution of Eq. (1) is

$$\Delta T(x) = \left[1 - \frac{\cosh(mx)}{\cosh(mL/2)}\right]\frac{IV}{\beta ALm^2} + \frac{\Delta T_1 + \Delta T_2}{2}\frac{\cosh(mx)}{\cosh(mL/2)} + \frac{\Delta T_2 - \Delta T_1}{2}\frac{\sinh(mx)}{\sinh(mL/2)}, \tag{2}$$

where ΔT_1 and ΔT_2 are the measured nanotube temperatures at the two metal contacts, and $m \equiv \sqrt{g\pi d/\kappa A}$.[8] Using the $\beta \equiv \kappa/\alpha$ value measured in vacuum at a similar average temperature in the nanotube, we vary m in Eq. (2) to fit the temperature profile measured in different gases. The fraction of heat dissipation to surrounding gas (Q_g) can be calculated from the temperature profile as

$$\frac{Q_g}{Q} = 1 - \frac{2\left(1 - \frac{\Delta T_1 + \Delta T_2}{2}\frac{\beta ALm^2}{IV}\right)\tanh\left(\frac{mL}{2}\right)}{mL}. \tag{3}$$

The results show that about 50%–60% of the Joule heating along the suspended nanotube is dissipated to the different

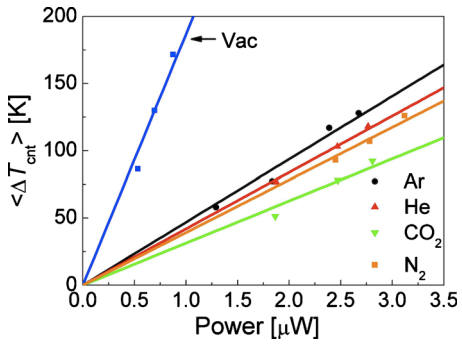

FIG. 4. (Color online) Average temperature of the CNT measured in different gases plotted with respect to power in different environments.

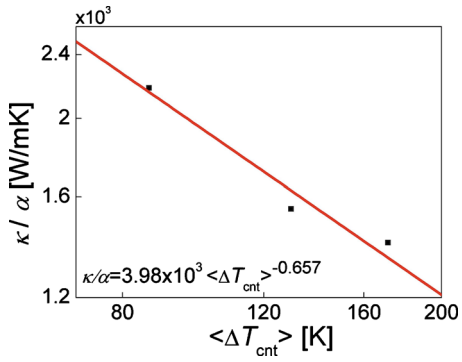

FIG. 5. (Color online) Measured k/α as a function of the average CNT temperature, $\langle \Delta T_{cnt}\rangle$, extracted from G band downshifts measured during electrical heating.

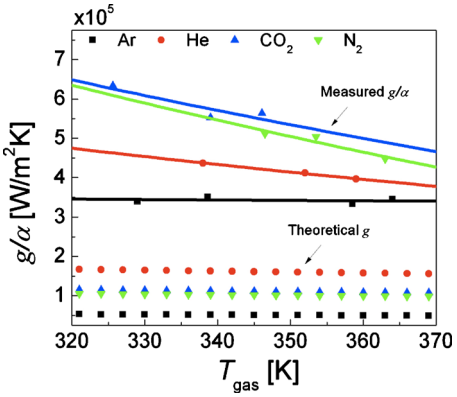

FIG. 6. (Color online) Measured g/α as a function of the gas temperature $T_{\text{gas}} \equiv \langle \Delta T_{\text{cnt}} \rangle / 2 + 300$ K. Solid lines show $T_{\text{gas}}^{-1/2}$ fitting to the measurement results (symbols). The symbols without the fitting lines are the theoretical g values from kinetic theory, proportional to $T_{\text{gas}}^{-1/2}$.

gases. Based on the m and β values, we further obtain the g/α value, as shown in Fig. 6 together with the maximum theoretical g values calculated from the kinetic theory with the accommodation coefficient equal to 1. If the electrical contact resistance is ignored and α is taken as 1, the measured g would be several times larger than the maximum theoretical value. Despite the uncertainty in α and g, the measurement results show a higher g value for CO_2 than He, which is opposite to the trend shown by the maximum theoretical values. Although the accommodation coefficient on the CNT surface could be higher for CO_2 than for He, further studies are required to clarify this discrepancy.

In addition, we have estimated the thermal contact resistance between the nanotube and an electrode as $R_c = (\Delta T_1 + \Delta T_2)/IV$, which is on the order of 10^8 K/W. This value is comparable to those reported for as-grown chemical-vapor deposition CNTs between two microthermometer devices.[21]

III. CONCLUSION

In this measurement, approximately half of the Joule heat generated in suspended CNTs is dissipated to the surrounding gas molecules from the likely defective current-carrying CNTs measured here. In addition, a higher thermal boundary conductance was measured in CO_2 than in He, which suggests a higher heat exchange rate between the CNT and the polyatomic molecules than that with monatomic molecules. The measurement results highlight the need of a vacuum environment for accurate measurement of the thermal conductivity of nanotubes and also graphene. With the availability of long suspended nanotube samples where the contact electrical resistance can be ignored and the hot phonon effect can be minimized in a low electric field, the method presented here can be used to obtain the molecular thermal boundary conductance between various gas molecules and nanotubes of different diameters.

ACKNOWLEDGMENTS

The authors would like to thank Dr. Junichiro Shiomi for useful discussions. This research was supported in part by DOE Award Nos. DE-FG02-07ER46376 and DE-FG02-07ER46377, and NSF Award No. CBET-0854118.

[1] S. J. Tans, M. H. Devoret, H. J. Dai, A. Thess, R. E. Smalley, L. J. Geerligs, and C. Dekker, Nature (London) **386**, 474 (1997).
[2] M. F. Yu, B. S. Files, S. Arepalli, and R. S. Ruoff, Phys. Rev. Lett. **84**, 5552 (2000).
[3] S. Berber, Y. K. Kwon, and D. Tomanek, Phys. Rev. Lett. **84**, 4613 (2000).
[4] Z. Yao, C. L. Kane, and C. Dekker, Phys. Rev. Lett. **84**, 2941 (2000).
[5] E. Pop, D. Mann, J. Cao, Q. Wang, K. Goodson, and H. J. Dai, Phys. Rev. Lett. **95**, 155505 (2005).
[6] A. W. Bushmaker, V. V. Deshpande, S. Hsieh, M. W. Bockrath, and S. B. Cronin, Nano Lett. **9**, 2862 (2009).
[7] M. Steiner, M. Freitag, V. Perebeinos, J. C. Tsang, J. P. Small, M. Kinoshita, D. N. Yuan, J. Liu, and P. Avouris, Nat. Nanotechnol. **4**, 320 (2009).
[8] L. Shi, J. H. Zhou, P. Kim, A. Bachtold, A. Majumdar, and P. L. McEuen, J. Appl. Phys. **105**, 104306 (2009).
[9] D. Mann, E. Pop, J. Cao, Q. Wang, K. Goodson, and H. J. Dai, J. Phys. Chem. B **110**, 1502 (2006).
[10] I. K. Hsu, R. Kumar, A. Bushmaker, S. B. Cronin, M. T. Pettes, L. Shi, T. Brintlinger, M. S. Fuhrer, and J. Cumings, Appl. Phys. Lett. **92**, 063119 (2008).
[11] V. V. Deshpande, S. Hsieh, A. W. Bushmaker, M. Bockrath, and S. B. Cronin, Phys. Rev. Lett. **102**, 105501 (2009).
[12] A. A. Balandin, S. Ghosh, W. Z. Bao, I. Calizo, D. Teweldebrhan, F. Miao, and C. N. Lau, Nano Lett. **8**, 902 (2008).
[13] Q. W. Li, C. H. Liu, X. S. Wang, and S. S. Fan, Nanotechnology **20**, 145702 (2009).
[14] M. Hu, S. Shenogin, P. Keblinski, and N. Raravikar, Appl. Phys. Lett. **90**, 231905 (2007).
[15] J. E. A. John, *Gas Dynamics* (Allyn and Bacon, Boston, 1933).
[16] A. W. Bushmaker, V. V. Deshpande, M. W. Bockrath, and S. B. Cronin, Nano Lett. **7**, 3618 (2007).
[17] S. M. Bachilo, M. S. Strano, C. Kittrell, R. H. Hauge, R. E. Smalley, and R. B. Weisman, Science **298**, 2361 (2002).
[18] F. M. Huang, K. T. Yue, P. H. Tan, S. L. Zhang, Z. J. Shi, X. H. Zhou, and Z. N. Gu, J. Appl. Phys. **84**, 4022 (1998).
[19] A. Bassil, P. Puech, L. Tubery, W. Bacsa, and E. Flahaut, Appl. Phys. Lett. **88**, 173113 (2006).
[20] N. Mingo and D. A. Broido, Phys. Rev. Lett. **95**, 096105 (2005).
[21] M. T. Pettes and L. Shi, Adv. Funct. Mater. **19**, 3918 (2009).